JTTEE5 11:266-275

Solidification Modeling of Plasma Sprayed TBC: Analysis of Remelt and Multiple Length Scales of Rough Substrates

Donald E. Wroblewski, Rajesh Khare, and Michael Gevelber

(Submitted 28 August 2000; in revised form 14 December 2000)

A two-dimensional, finite-element model based on an enthalpy formulation, was developed to simulate a splat solidifying on a rough substrate (with an idealized, sinusoidal-shaped roughness) capturing the multiple-length scales seen in real coatings as well as different aspect ratios. The model was used to study the effects of substrate temperature, splat temperature, and roughness characteristics on the onset and extent of remelt. Remelt is studied since it is indicative of local heat transfer conditions and might explain observed coating properties. Multiple splats were simulated using the two-dimensional model for short-time cooling coupled to a one-dimensional model for long-time cooling to predict substrate temperature rise prior to subsequent splat impacts. The presence of roughness promoted substrate remelting at conditions under which no remelting was observed for a smooth surface, suggesting that substrate roughness is an important parameter to include in splat solidification studies. The effects of splat temperature and substrate temperature on remelt were consolidated into a single nondimensional parameter, which captured a number of critical phenomena including characterization of the onset of remelt with a nondimensional remelting point.

Keywords microstructure formation, solidification modeling, splat remelt, splat solidification, substrate roughness, thermal barrier coatings

1. Introduction

Direct current (DC) arc plasma deposition has been an enabling technology in many applications (e.g., aerospace, engines, and power generation) due to its ability to economically manufacture coatings with desired properties. For example, ceramic thermal barrier coatings (TBCs), which have desirable porosity, microcracks, thermal conductivity, and adhesion, are routinely sprayed onto engine surfaces to protect the underlying components from damage by hot combustion gases. Developing the capability to customize coatings through more direct control of microstructure will potentially open new markets for DC spraying and will expedite the evolution of the next generation of coating technologies.

Splat solidification dynamics is a major driving force in determining the resulting coating structure (e.g., composition, splat shape, cracks, and voids). While previous modeling and experimental research has been reported on this critical phenomenon, little of this work has focused on the impact of surface roughness. The analysis reported here examines the role of surface roughness in terms of the variety of aspect ratio and length scales observed for real sprayed surfaces. A major focus of this analysis is the degree of remelt, since it is believed to be important for explaining observed cracking and grain structures, as well as being an easily observed indicator of the local heat transfer.

A major microstructural feature of TBCs is porosity, including horizontal cracks or delaminations, vertical cracks, and voids with no preferred direction. Important characteristics include the size, orientation, and distribution of this porosity, which are influenced greatly by the thermal environment associated with the spreading of sprayed droplets into splats on the surface and the subsequent rapid solidification. In particular, critical conditions include particle state at impact (temperature and velocity), which is controlled by torch operating characteristics, the torch-substrate standoff distance, and the substrate temperature.[1] Thus, a prerequisite for engineering coatings through direct control of the coating microstructure is a fundamental understanding of the splat-substrate interfacial heat transfer associated with the spreading and rapid solidification. This article concentrates on developing a deeper understanding of the solidification dynamics that are critical to determining these features. In particular, it addresses a critical factor that, to our knowledge, has not been adequately considered—the impact of multiple-scale roughness.

1.1 Horizontal Delaminations

The results of this research are particularly important for understanding the formation of horizontal cracks, which will be referred to here as horizontal delaminations, the thin gaps oriented mainly normal to the direction of spraying. These delaminations may be observed between individual splats—*intersplat delaminations*, which are about 0.01 μm in thickness—or between lamella of four to seven splats built up during a single pass of the torch—*interlamellar delaminations*, which are about 0.2 μm in thickness and are seen quite prominently in the micrographs of coatings.[2] The horizontal delaminations are impor-

Donald E. Wroblewski, Rajesh Khare, and **Michael Gevelber,** College of Engineering, Boston University, Boston, MA 02215. Contact e-mail: dew11@bu.edu.

tant for two reasons. First, their presence near the bond coat can reduce bond strength, compromising the reliability of the coating during operation. Second, their orientation normal to the flow of heat in TBCs leads to a reduction in thermal conductivity and thus increases the thermal resistance properties of the coating.[3-5]

The focus of the present work was motivated by results from two studies involving microstructural characterizations of TBC. Bengtsson and Johannesson[2] showed that the density and distribution of the horizontal delaminations was a strong function of the substrate temperature. At lower temperatures, both interlamellar delaminations (i.e., between lamellae from successive passes of the spray torch) and intersplat delaminations (i.e., between individual splats in one pass) were observed. However, at higher substrate temperatures, only interlamellar delaminations were prominent. In addition, grains were observed to grow vertically through different splats. This was surprising given that the mean time between successive splats during a pass was expected to be on the order of 10 ms, which is several orders-of-magnitude beyond the solidification time of a single splat. Further, a one-dimensional model of splat cooling indicated that a previously solidified splat would not remelt when struck by a subsequent splat, raising the question of why the grains grow across splat boundaries.

McPherson[6] showed that the coating microstructure consists of splats having a limited number of contact points. It was experimentally shown that the true contact area between splats/lamellae, which is circular in shape, is only about 20% of the splat area. The area between these contact points represents the delaminations.

The results of both of these studies are consistent with the idea that horizontal cracks form because of the curling of the edge of the solidified splats[7] due to thermal quenching stress[8] during rapid cooling.

However, this article will explore another contributing factor that may be important: that the delaminations naturally occur between splats except where the early phase of splat cooling has promoted remelting of the underlying substrate. The contact points may be regions near the peaks of roughness features where remelting will first occur, causing circular-shaped "spot welds" between splats. At higher substrate temperatures, a larger portion of the substrate becomes remelted, creating an increased area of true contact and a corresponding decrease in the delamination area. Remelting also could be a factor in explaining the observed columnar grain structure between splats.

Nomenclature

A	roughness height—peak-to-valley [m]
C	constant used in remelt correlation equation
C_p	specific heat [kJ/kg K]
D	splat thickness [m]
h	enthalpy [kJ/kg]
h_s	enthalpy of solid at melting temperature [kJ/kg]
h_{sf}	enthalpy of fusion [kJ/kg]
$\overline{h}$	nondimensional enthalpy $\frac{h - h_s}{h_{sf}}$
$[K]$	nondimensional "stiffness" matrix
$[M]$	nondimensional "mass" matrix
P	depth of solution domain in substrate [m]
R	extent of remelt S_{melt}/S
R_m	maximum remelt
S	length of interface from peak-to-valley [m]
S_{melt}	length of interface that is remelted [m]
Ste	Stefan number $\frac{C_p(T_{spl} - T_m)}{h_{sf}}$
t	time [s]
t_m	time to maximum remelt [s]
T	temperature [K]
T_m	melting temperature [K]
T_{spl}	initial splat temperature [K]
T_{sub}	initial substrate temperature [K]
U	nondimensional temperature parameter $\frac{T_{spl} - T_m}{T_{spl} - T_{sub}}$
U_{remelt}	nondimensional remelting point
W	width of roughness— peak-to-valley [m]
x, y	coordinates [μm]
$\overline{x}, \overline{y}$	nondimensional coordinates x / D, y / D
α	thermal diffusivity [m^2/s]
θ	nondimensional temperature $\frac{T - T_m}{T_{spl} - T_m}$
θ_{sub}	nondimensional initial substrate temperature
τ	nondimensional time $\frac{t}{D^2/\alpha}$

1.2 Interfacial Roughness Effects

The study of the substrate remelting phenomenon requires an understanding of the critical physical processes associated with splat flattening and cooling. For zirconia TBCs, a number of experimental and numerical research efforts[1,9,10] have focused on single splat impacts. However, the experimental efforts often involve spraying onto polished substrates. Likewise, the modeling efforts incorporate a particle impacting and/or a splat cooling on a smooth surface, with the interface heat transfer modeled using a macroscopic thermal contact resistance. The contact resistance normally is chosen empirically to obtain the best fit between the modeled surface temperature evolution and the measured splat surface temperature measurements.[1,10,11]

This study addresses the effect of realistic surfaces, which are observed to be rough. This includes the first several layers on the bond coat and throughout the TBC. In this light, previous experimental and modeling studies have focused on surfaces that are likely not to be characteristic of deposition throughout the majority of the spray process. For example, scanning electron microscope (SEM) micrographs of the surface of a zirconia coating (Fig. 1) reveal roughness features at different length scales, ranging from 10 μm down to 0.1 μm, with the latter likely to be features of individual grains.

This heterogeneous interface, with multiple-scale roughness, is what a molten drop encounters during splat formation and solidification, and, thus, the roughness characteristics may play an important role in microstructure formation. However, most past efforts addressing the issue have been either qualitative in nature[6,12] or focused mainly on void formation at impact[13-15] or on general splat features.[16] Little has been done to quantitatively investigate the effect of roughness on the solidification process.

While a major focus of this research is to investigate the possibility of remelting as an explanation for the observed depen-

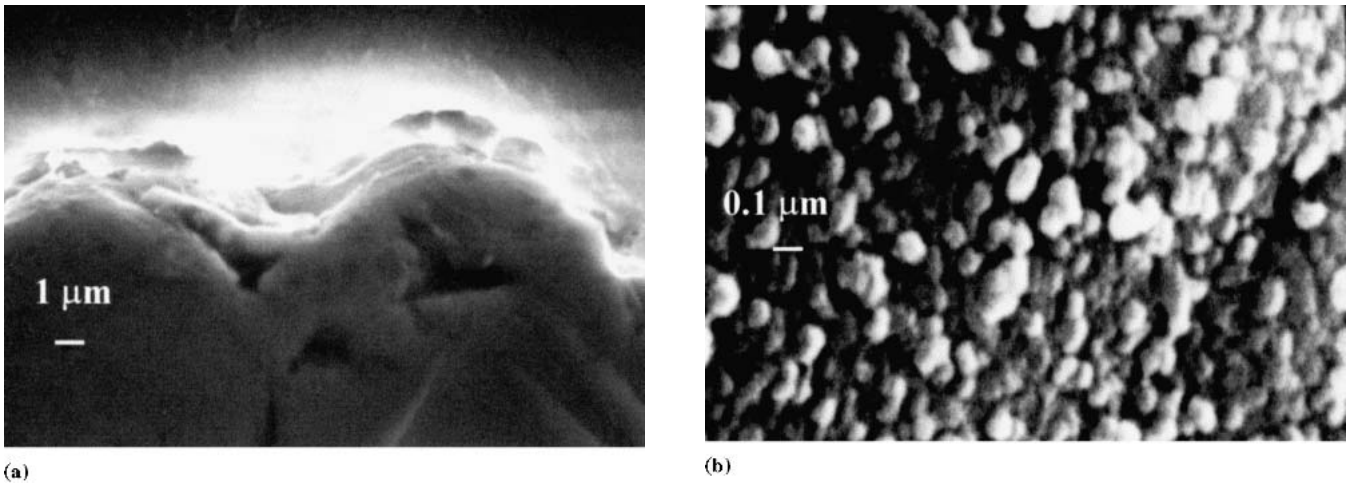

Fig. 1 Scanning electron microscope micrographs of plasma-sprayed, ytrria-stabilized zirconia coatings: **(a)** a polished cross-section exhibiting large-scale roughness (10 μm scale) and smaller scale features (1 μm scale); and **(b)** unpolished surface (top view) showing grain-level roughness (100 nm scale)

dence of delamination density on substrate temperature, roughness and remelting also may have importance for understanding other aspects of coating structure.

1.3 Objectives of Study

To capture the effect of a rough substrate, a two-dimensional model of splat cooling has been developed, featuring an idealized rough surface based on physical dimensions that have been obtained from experimental evidence, such as that seen in Fig. 1. This article will describe the use of the model to investigate the onset and extent of substrate remelting and how these are influenced by thermal conditions (i.e., substrate and splat temperature) and by the characteristics of the surface roughness (i.e., length scale of roughness and roughness aspect ratio). Here, the *onset* of remelt refers to the thermal conditions under which it is first observed, and the *extent* of remelt refers to the area of the interface that is remelted.

It should be noted that as splats build up during a single pass of the torch, the substrate surface temperature increases due to the inability of the relatively low thermal conductivity substrate to diffuse heat away from the cooling splat. Thus, a splat solidifying on a splat from the same torch pass may be a different event than the first splat in a pass solidifying on the splats built up from an earlier pass. This gives rise to the speculation that an interface that does not remelt with the first splat may remelt with subsequent splats. Therefore, this investigation also considers the effect of multiple splats during a single pass.

2. Problem Formulation

2.1 Model Geometry and Assumptions

As a molten particle encounters a rough substrate formed by previously deposited splats, it will spread over the peaks and valleys, and the result will be a hot splat sitting on the contours of the cooler surface. Figure 2 shows a schematic representing the idealized situations for two different roughness scales, which are the basis for the problem formulation. There are several simplifying assumptions that lead to this idealized geometry.

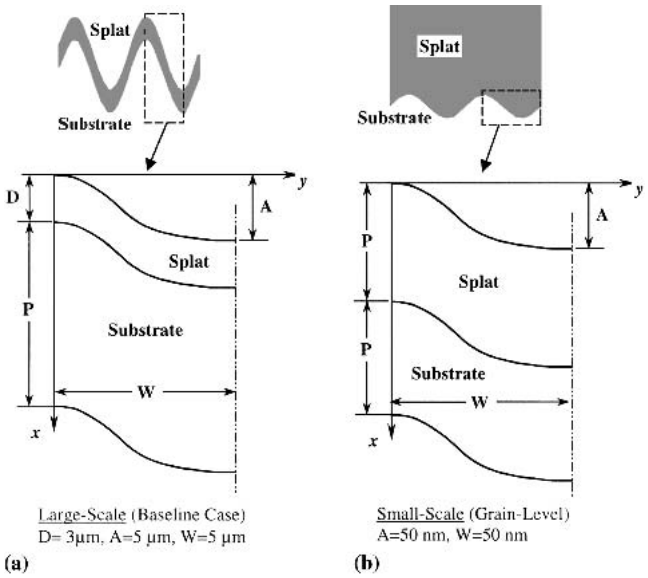

Fig. 2 Idealized roughness geometries and solution domains used for numerical analysis: **(a)** large-scale (baseline case); and **(b)** small-scale (grain-level)

First, the roughness is assumed to follow a two-dimensional sinusoidal profile. Although the two-dimensional roughness may exhibit different quantitative results than the more realistic three-dimensional roughness, the overall qualitative trends for remelting are expected to be similar.

Second, the spreading and solidification have been decoupled, so that the initial state for the simulations is an isothermal splat covering an isothermal substrate. This assumption is supported by numerical investigations showing spreading times

on the order of 0.4 μs and solidification times on the order of 10 μs.[17,18]

Third, perfect contact is assumed across the entire splat-substrate interface, whereas real interfaces are likely to feature incomplete filling of the troughs of the roughness. The effect of imperfect contact on remelt will depend on the size and thickness of the gaps near the troughs. However, under some conditions, it may lead to a greater extent of remelt than the perfect contact case, since the splat will cool more slowly, promoting more lateral heat transfer.

Finally, the splat is assumed to have a uniform thickness over the entire surface, whereas the real situation would likely exhibit nonuniform splat thickness. Despite these assumptions, the idealized problem should preserve the essential features of the interface transport that are affected by surface roughness. In addition, it is likely that these idealized assumptions, particularly the first and third, will lead to an underprediction of remelt and, hence, to conservative estimates of the effect of interface roughness.

Examinations of the surface of sprayed coatings (Fig. 1) have revealed that there are multiple-length scales present on the coating surface, which could affect solidification dynamics. In the present study, it is assumed that these roughness scales can be modeled by sinusoids of various aspect ratios and dimensions. These sinusoidal roughness profiles are assumed to be periodic, so the heat transfer model is applied to only a small section of the interface (Fig. 2). The following two cases are illustrated: (1) large-scale roughness, representing the base case for the analysis, for which the physical dimensions are A = 5μm and W = 5 μm; and (2) grain-level roughness, for which A = 50 nm and W = 50 nm. Note that the sinusoidal shape of the grain level roughness approximates the hemispherical shape observed in micrographs.

The depth P from the bottom of the splat to the bottom of the numerical domain is chosen based on the thermal penetration depth for the required time for the simulation, so that the bottom can be modeled as an adiabatic surface. Accordingly, $P = 4\sqrt{\alpha t} + A$, where α is the thermal diffusivity and t is the final time for the simulation—the time required to observe maximum remelt. Maximum remelt was found to occur when the remelting initiated at the peak of the roughness had spread to its maximum extent along the splat-substrate interface and the surface had begun to resolidify. This essential concept will be discussed in more detail below. For the grain-level roughness, maximum remelt occurs in a time less than the time required for heat to diffuse from the interface to the top of the splat. For that case, the problem can be treated as an interface separating infinite liquid and solid layers. Numerically, this is handled by setting the top of the splat domain at the same distance as the bottom of the substrate domain (Fig. 2b).

2.2 Governing Equations

The governing equation solved within the modeled splat domain was the two-dimensional transient conduction equation in enthalpy form. The scheme for solving the phase change problem here has been described in detail.[19] Assuming that the thermal conductivity and specific heat of the solid and liquid phases are equal and independent of temperature, the appropriate nondimensional form of the equation is as follows:

$$\frac{\partial \bar{h}}{\partial \tau} = (Ste)\frac{\partial^2 \theta}{\partial_x^{-2}} + (Ste)\frac{\partial^2 \theta}{\partial_y^{-2}} \tag{1}$$

where

$$Ste = \frac{C_p(T_{spl} - T_m)}{h_{sf}},$$

is the Stefan number. The pertinent nondimensional variables are as follows:

$$\theta = \frac{T - T_m}{T_{spl} - T_m}; \quad \bar{h} = \frac{h - h_s}{h_{sf}}; \quad \tau = \frac{t}{D^2/\alpha}; \quad \bar{x} = \frac{x}{D}; \quad \bar{y} = \frac{y}{D}; \tag{2}$$

where T_m is the equilibrium melting temperature, T_{spl} is the initial temperature of the splat, h_s is the solid enthalpy at the melting temperature, h_{sf} is the enthalpy of fusion, C_p is the specific heat, and D is the splat thickness. This formulation assumes that the thermal diffusivity is isotropic. In general, this is not true due to the porosity in the deposited coating that acts as the substrate. However, within the time frame associated with the critical two-dimensional effects that influence remelt, the thermal penetration depth is on the order of several splat thicknesses, over which porosity effects should be minimal.

The enthalpy temperature mapping required for solving Eq 1 assumes equilibrium melting, i.e., no undercooling, and no solid-solid phase change. In nondimensional form the mapping is as follows:

Solid Phase ($\bar{h} < 0$)	$\bar{h} = Ste\theta$	(3a)
Two Phase ($0 \le \bar{h} \le 1$)	$\theta = 1$	(3b)
Liquid Phase ($\bar{h} > 1$)	$\bar{h} = 1 + Ste\theta$	(3c)

There are four key nondimensional parameters in this problem as follows: *Ste*, the Stefan number; θ_{sub}, the nondimensional initial substrate temperature, which is a measure of the thermal driving force for solidification; *A/D*, the ratio of the roughness height and splat thickness; and *A/W*, the aspect ratio of the roughness. The Stefan number can be interpreted as the ratio of a diffusion time scale to a melting/solidification time scale. For conditions typical of TBCs, the Stefan number is on the order of one, suggesting that the diffusion and phase change effects are comparable.

Adiabatic conditions are assumed at all boundaries. For the transverse boundaries of the domain, this is valid because of the periodic nature of roughness profiles. For the bottom, it is valid based on the choice of the domain size for the substrate, as described above. For the top surface, it is valid since convection and radiation from the surface are negligible compared to the high conduction rates at the interface.[20]

2.3 Numerical Approach

A finite element method was chosen over a finite difference scheme so that the domain approximation error associated with the geometric modeling of the curved interface surface could be minimized. The finite element model was developed using the weak form with linear rectangular elements, a first-order inter-

polation function, and a forward difference scheme in time as follows:

$$[M]\frac{\{\bar{h}\}^{n+1}-\{\bar{h}\}^{n}}{\tau}=-[K]\{\theta\}^{n} \quad (4)$$

where [*M*] is the "mass" matrix and [*K*] is the "stiffness" matrix.

Equation 4 was solved in two steps. In the first step, the matrices were developed for a specific set of conditions using (Computer Aided Learning of the Finite Element Method) CALFEM, a toolbox for MATLAB (MathWorks, Inc., USA). In the second step, the matrices from CALFEM script were solved using LU decomposition. Both steps were carried out on an SGI (Mountain View, CA) Origin2000 computer. The required computation time for the first step using the final refined grid, with 2000 elements within the splat, was about 16 h, and that for the second step was about 4 h.

The mesh used for the simulation was specified on a rectangular domain and then was transformed into the sinusoidal domain. A detailed mesh refinement analysis was carried out.[20] The critical factor in selecting the grid size was minimizing the remelt-front jumping. If the grid were too coarse, the remelt front would jump from one grid point to the next in subsequent time steps or in subsequent changes in the substrate temperature or splat temperature for different runs. A grid-independent solution was achieved with 100 unevenly spaced grid points in the splat in the direction normal to the interface and 100 evenly spaced grid points in the splat in the direction along the interface. The uneven grid structure featured smaller elements in both the splat and the substrate near the interface to capture the steep temperature and enthalpy gradients associated with the early-time, interface heat transfer.

As a check on the validity of the model, the total enthalpy within the domain was monitored; since all boundaries were adiabatic, the enthalpy should have remained constant with time. Over 10 μs (approximately the time scale associated with maximum remelt), the total enthalpy as calculated from simulation results did not change by more than 0.7% (T_{spl} = 3773 K; T_{sub} = 1073 K; 3 μ*m* thick splat).

2.4 Simulation of Multiple Splats

Using the two-dimensional model to simulate the cooling of a single splat until the next splat arrived would be computationally expensive because of the large domain required. Assuming the time between splats is 10 ms,[18] the thermal penetration depth, and hence the domain length, would be approximately 150 times the thickness of the splat, for just one splat. However, at about 100 μs, an isotherm plot of the splat-substrate domain from the two-dimensional simulation showed that the splat was completely solid and that the temperature profile was almost one-dimensional; the isotherm plots in Fig. 3 illustrate how the temperature field evolves toward one-dimensional behavior. Thus, it can be concluded that while the solidification exhibits short-time two-dimensional behavior, the long-time cooling process is essentially one-dimensional.

With this in mind, a one-dimensional model of a splat cooling on a smooth surface was used to estimate the rise in the substrate temperature with multiple splats. The model employed a finite difference scheme applied to the one-dimensional form of Eq 1. The depth of the substrate domain for the simulation was set so that it was greater than the penetration depth for the total time for all four splats to be considered in a single pass. This domain extended over a range of hundreds of previously deposited splats, and thus the diffusion process would likely be affected by the coating porosity. To account for this porosity effect, the thermal diffusivity was set at 30% of the value for solid zirconia[4,21] for the one-dimensional analysis.

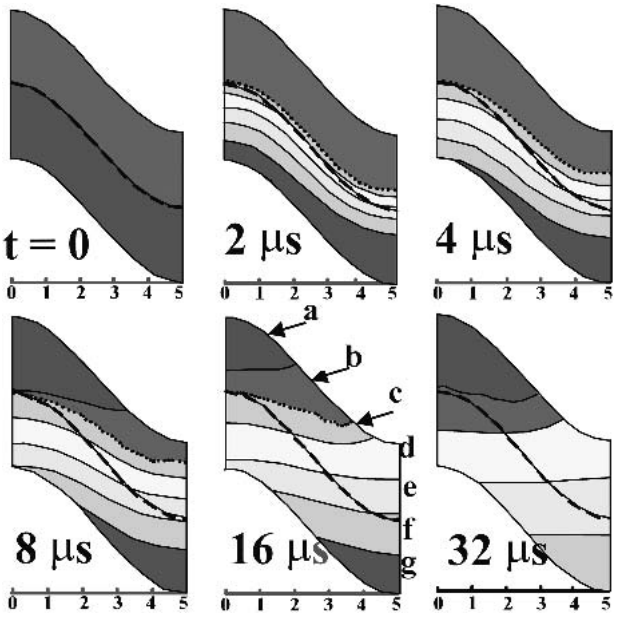

Fig. 3 Evolution of isotherms for baseline case. The dashed line represents the initial interface. The dotted line is the melting temperature contour. a, >3000 K; b, 2850 to 3000 K; c, 2700 to 2850 K; d, 2300 to 2700 K; e, 1900 to 2300 K; f, 1500 to 1900 K; g, 1100 to 1500 K. Only partial domain shown for substrate

The first splat was allowed to solidify and cool for 10 ms (i.e., 10,000 μs) on an initially isothermal substrate. Then, the top of the first splat was set as the surface of the substrate for the second splat. With the substrate temperature initialized to the temperature profile from the end of the simulation of the first splat, the cooling of the second splat was simulated. This was repeated to simulate the buildup of four splats. The results of these one-dimensional simulations of multiple splats then were used as input to predict remelt on a rough substrate, as described in more detail below.

3. Results and Discussion

3.1 Baseline Case

Although the problem was formulated and the numerical method was programmed and solved in a nondimensional form, the results will be discussed mainly in a dimensional form to better focus the discussion on the TBC application. An evaluation of the results in a nondimensional form also is presented.

The parameters for the base case were as follows: D = 3 μm; T_{spl} = 3773 K (both chosen based on the experimental observations from Ref. 1); T_{sub} = 1073 K (the high substrate temperature

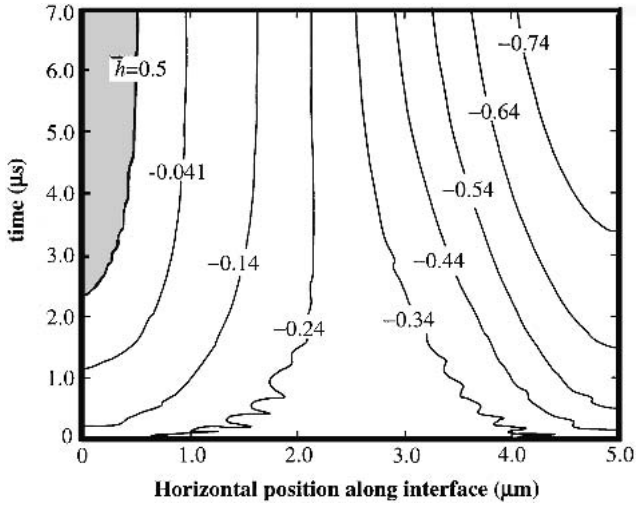

Fig. 4 Time history of nondimensional enthalpy, $\bar{h} = (h - h_s)/h_{sf}$, along the initial splat-substrate interface

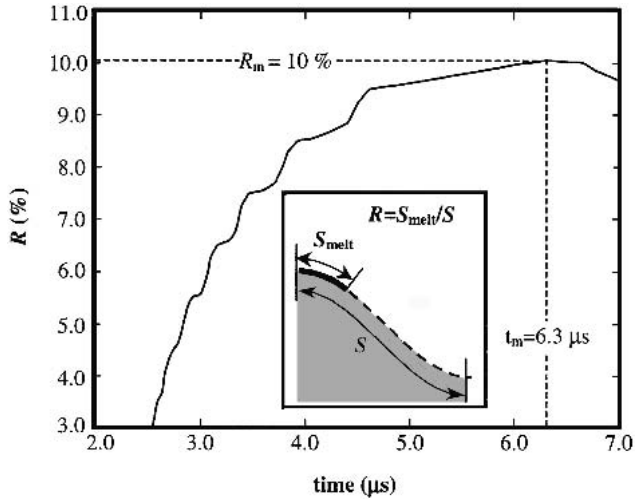

Fig. 5 Extent of remelt, R, as a function of time for baseline case. Note maximum remelt, R_m, at 6.3 μs

case reported in Ref. 2); A = 5μm; and W = 5 μm (large-scale roughness as seen in Fig. 1). Based on the properties of zirconia, the nondimensional parameters for the base case were as follows: Ste = 0.70; A/W = 1; A/D = 1.67; and θ_{sub} = 2.28.

The results for the baseline case are shown in Fig. 3, representing snapshots of the isotherms in the splat and substrate near the interface for different times. (Note that only a portion of the substrate domain is shown.) The dashed line represents the initial splat-substrate interface, and the dotted line shows the isotherm for the melting temperature. As the splat solidifies, the solidification front proceeds from the valley of the roughness to the peak of the splat. Eventually, the substrate begins to remelt near the peak of the roughness (between 2 and 3 μs) and later begins to resolidify. Such remelting is attributed to the lateral heat flux from the splat to the substrate, which is not captured with a one-dimensional model of a smooth substrate. Also, note that after 32 μs, the splat cooling is approaching one-dimensional behavior.

To better observe the phenomena of interface remelting, the thermal history of the interface is shown in Fig. 4 as a time-position contour plot of enthalpy. Note that the melt front is interpreted as the spatial location where the nondimensional enthalpy is 0.5. The remelting begins at the peak of the roughness at about 2.3 μs, then spreads along the interface until reaching its maximum extent at about 6.3 μs, and finally begins to recede as the remelted part of the interface resolidifies.

The extent of the remelt, R, at a specified time is defined as the percentage of the interface area that is remelted at that time, as determined by the position of contour, as shown in the insert in Fig. 5. Also shown in Fig. 5 is the variation of R with time for the baseline case, exhibiting a maximum remelt of R_m = 10% at time t_m = 6.3 μs. Figures 4 and 5 represent the behavior of the initial splat-substrate interface, but they do not display the extent to which the remelt has penetrated into the substrate normal to the interface. At the time of the maximum remelt, this penetration was found to be approximately 0.095 μm at the peak of the roughness, which is less than 2% of the peak-to-valley roughness height.

Note that the solution displays an initial instability that decays with time, which is seen most clearly in the contour in Fig. 4. This problem is known to be inherent in the enthalpy scheme[19] and can be corrected to some extent by tracking the temperature or enthalpy only when the melt front crosses a node.[22] Moreover, the solution at longer times has been proved to be correct and accurate,[19] so that the maximum remelt results should not be affected by this instability.

3.2 Thermal Effects

Figure 6 shows the effect of substrate temperature on the maximum extent of remelting, R_m. The onset of remelting is observed at approximately 600 °C. For higher substrate temperatures, the maximum remelt increases with the substrate temperature, implying that the intersplat bonding due to welding at the interface increases with higher substrate temperatures. In Fig. 7, the same results are plotted as $1 - R_m$, the percentage of the interface that does not remelt, and are compared to the observations of delamination density from Ref 2. Note that the numerical results are for the first splat in the pass and for a single splat thickness, splat temperature, and roughness geometry. As such, the comparison is meant to be only qualitative. The two show similar trends, which is consistent with the idea that the variation in delamination density with substrate temperature is due to variations in the extent of remelt. In particular, the delamination density is unchanged at lower substrate temperatures, which are conditions at which no remelt is predicted, and decreases at higher substrate temperatures, which are associated with an increasing extent of remelt.

As seen in Fig. 8, increasing splat temperature has an effect that is similar to that of increasing substrate temperature. The onset of remelt occurs between 3400 and 3450 °C, and the extent of remelt increases for higher splat temperatures. The implication from these results is that the remelting phenomenon, and hence possibly the microstructural features, can be controlled by varying the substrate, or the splat temperature, or both.

It is useful to analyze the thermal effects on remelt using a

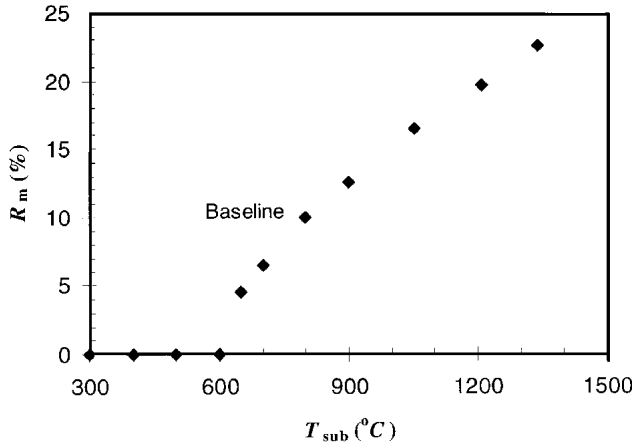

Fig. 6 Effect of substrate temperature on remelt (T_{spl} = 3500 °C)

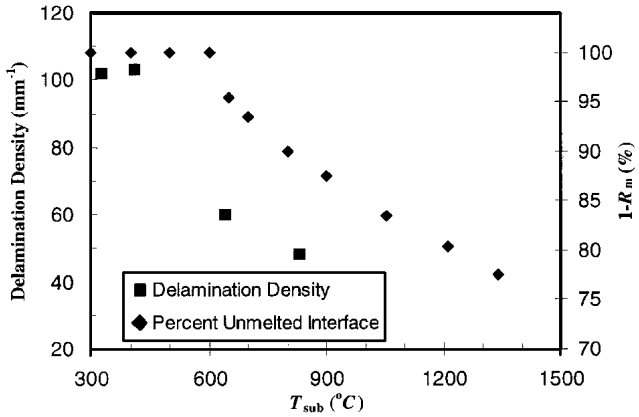

Fig. 7 Comparison of numerical results (percentage of interface not remelted) with delamination density measurements (Ref 2)

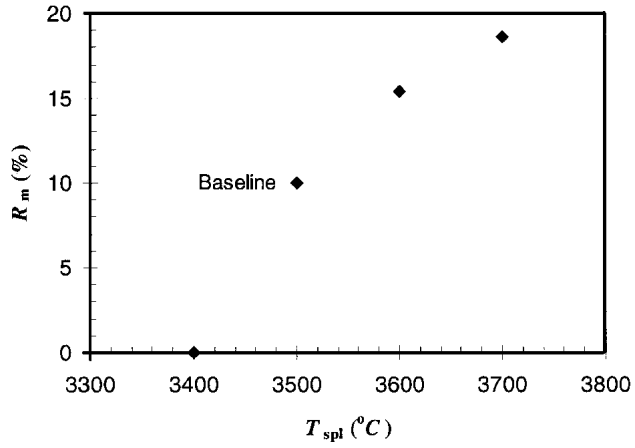

Fig. 8 The effect of splat temperature on the extent of remelt (T_{sub} = 800 °C)

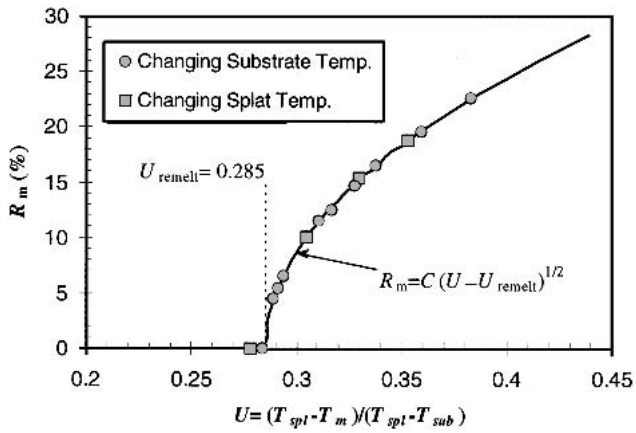

Fig. 9 The extent of remelt as a function of nondimensional thermal parameter, U, accounting for substrate temperature changes and splat temperature changes

nondimensional temperature parameter, $U = (T_{spl} - T_m)/(T_{spl} - T_{sub})$, which is related to the nondimensional initial substrate temperature, $U = 1/(1 - \theta_{sub})$. Note that for a fixed melting temperature, increasing values of U are associated with increasing splat temperatures at a fixed substrate temperature and with increasing substrate temperatures for a fixed splat temperature. Figure 9 shows R_m as a function of U for the cases of changing substrate temperature and changing splat temperature. The data can be correlated with a single curve, indicating that changing splat temperature and substrate can be combined into a single parameter. Note that substrate remelting occurs only above a certain value of U. This can be defined as the nondimensional "remelting point," U_{remelt}, which should be a function of the material properties and of the roughness and splat geometry. For this case, the remelting point has a value of 0.285. For thermal conditions corresponding to values of U above the nondimensional remelting point, the substrate will remelt and the area of interface remelted increases with increasing U above the remelting point according to a curve of the form $R_m = C(U - U_{remelt})^{1/2}$, where $C = 72.0$ for this case. This relationship will subsequently be referred to as the remelt curve. Note that for the one-dimensional case, the remelt curve is a step function that is characterized by a nondimensional remelting point of 0.5 and a remelting of the entire surface (R_m = 100%) for $U > 0.5$.

The extent of remelt shown by the remelt curve in Fig. 9 is approaching 20%, which is consistent with the other observations of a 20% true contact area for zirconia coatings.[6] Although this level of remelt is seen only for the highest values of U, it is expected that the actual values of R_m will be higher than the numerical predictions. This is because the assumptions and idealizations adopted for this study will tend to underpredict the extent of remelt (as discussed above).

The results presented in Figs. 6 and 8 indicate that changing the splat temperature by some fixed amount (say, 100 °C) has a greater effect on the extent of remelting than does changing the substrate temperature by the same amount. Using the remelt curve shown in Fig. 9, this can be proven in a more general sense as long as $U < 0.5$, which represents the regime for the thermal conditions that are likely to be encountered for zirconia-based TBCs. However, from a control point of view, it may be easier to control substrate temperature over a large range than it would be to control splat temperature, thus providing greater control authority.

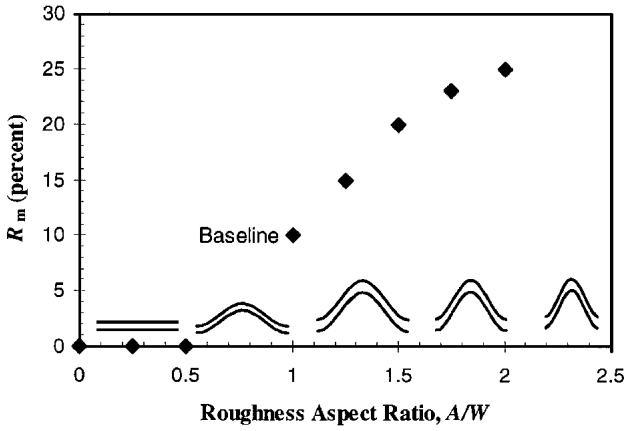

Fig. 10 The extent of remelt as a function of roughness aspect ratio, A/W (T_{spl} = 3500 °C, T_{sub} = 800 °C)

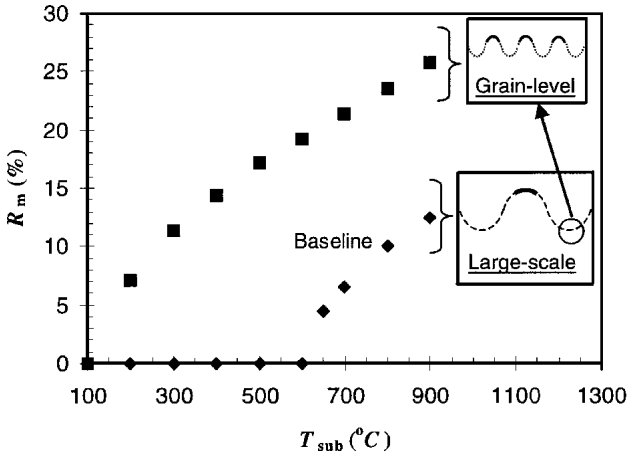

Fig. 11 The effect of substrate temperature on the extent of remelt for grain-level roughness, $A = W$ = 50 nm, with comparison to large-scale roughness, $A = W$ = 5 μm (T_{spl} = 3500 °C)

3.3 Roughness Effects

The effect on remelt of the aspect ratio of the substrate roughness is shown in Fig. 10 for the baseline thermal conditions. The cases for an aspect ratio greater than 1 involved increasing the wavelength for a fixed roughness height (i.e., 5 μm), while the cases for an aspect ratio less than 1 involved decreasing roughness height for a fixed wavelength. No remelting occurs for the case of flat substrates or for roughness aspect ratios up to 0.5, and the extent of remelt increases with increasing aspect ratios above 0.5. Since remelting occurs mainly because of the early-time, two-dimensional heat transfer near the roughness peak, this effect should be more pronounced as the local radius of curvature near the peak is reduced with larger aspect ratios. As such, the remelting point is expected to decrease with increasing aspect ratios.

The effect of substrate temperature for the small-scale roughness is compared to that of the larger scale roughness in Fig. 11. The onset of remelt occurs at a much lower substrate temperature for the smaller scale roughness, and the extent of remelt is at least twice that at the larger scales for a given substrate temperature. As discussed above, the splat thickness is irrelevant for the smaller scale roughness, since the time scale in which remelting occurs is much smaller compared to the thermal penetration time for the splat thickness. Hence the splat domain seen by the interface is a semi-infinite splat, and the moving solidification front is not inhibited by the splat thickness. Thus, the results shown in Fig. 11 are valid for smaller scale roughness as well and also for larger scale roughness up to the scale for which the time that maximum remelt occurs is approximately the same as the diffusion time associated with the splat thickness.

As a point of clarification, it is important to note that R_m represents the percentage of the interface remelted for the "unit roughness," not for the entire interface. So, as shown in the drawings in Fig. 11, the specified extent of remelt for the two different cases is defined relative to the pertinent roughness scales. A larger extent of remelt for the grain-level roughness means that a larger fraction of the small-scale roughness interface will remelt compared to the large-scale roughness interface under the same conditions.

It is interesting to consider the interaction between the two different scales. Over the length scale of the small-scale roughness, remelt and solidification occur within nanoseconds. Since this time is much less than the time scale associated with the two-dimensional effects over the large-scale roughness, it is expected that the degree of initial remelting on the grain-level roughness should not depend on the location along the large-scale roughness. Therefore, as implied in the drawings in Fig. 11, remelt at the grain level will occur even in regions of the trough of the large-scale roughness. However, as the large-scale effects emerge within the microsecond time frame, additional remelt occurs in regions near the peak of the large-scale roughness. This remelt has a depth of penetration of approximately 100 nm, which is larger than the grain-level roughness, so in the region where large-scale remelt occurs, the entire grain-level roughness along with its interface is remelted. In the region near the troughs, where no remelting is observed at the large scale, the grain-level remelt pattern should be preserved.

Although only the substrate temperature was varied for the small-scale roughness simulations, the results still can be considered in the form of the nondimensional parameter U and the data can be fit to a remelt curve of the form $R_m = C(U - U_{remelt})^{0.5}$. In this case, $C = 95.4$ and $U_{remelt} = 0.244$, compared to $C = 72.0$ and $U_{remelt} = 0.285$ for the large-scale roughness. This equation is plotted in Fig. 12 along with the corresponding equation for the large-scale roughness. Also shown is the behavior for a flat surface—i.e., a step-function remelt curve with a nondimensional melting point of 0.5. Compared to the large-scale roughness, the small-scale roughness will exhibit the onset of remelt at a lower value of U—i.e., at lower substrate and splat temperatures—and there will be a greater extent of remelt for a given increase in the nondimensional parameter U above the remelting point. Compared to the smooth case, both rough surfaces exhibit a lower remelting point.

To compare the behavior of the rough and smooth surfaces, it is necessary to extrapolate the rough surface equations beyond the conditions simulated in this study, up to the remelting point of the smooth surface ($U = 0.5$). As seen in Fig. 12, the small-scale roughness shows that approximately 50% of the interface is remelted at that point, meaning that the remelt zone extends to

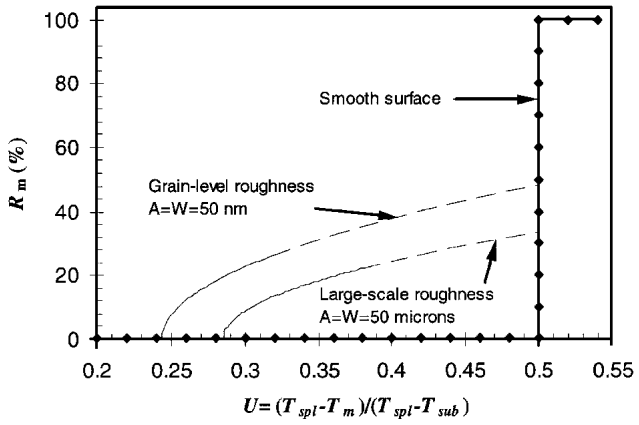

Fig. 12 Comparison of nondimensional melting behavior for large-scale roughness, grain-level roughness, and smooth surface cases. Dashed lines represent extrapolation of the curves.

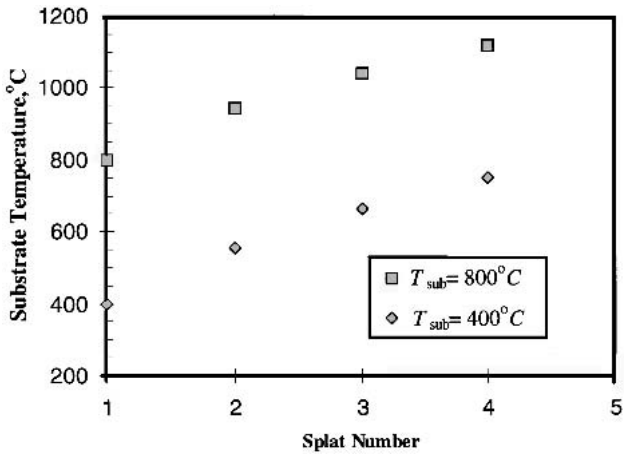

Fig. 13 Substrate temperature for each of the four splats in a single pass (T_{spl} = 3500 °C; 10 ms between splats)

the point where the curvature of the substrate surface is zero. This result is expected, since the two-dimensional effects, which drive the onset of remelt, will be negligible at the flat substrate surface midway between the peak and the valley of the roughness. Thus, that region should not remelt until the remelting point of the smooth surface is achieved (U = 0.5). Beyond that point, in the trough of the roughness, higher values of U are required to induce remelt, since two-dimensional effects in this region will tend to drive the interface away from an early onset of remelt and toward an early onset of solidification.

3.4 Multiple Splats

Figure 13 shows the substrate temperature predicted by the one-dimensional simulations for two different initial substrate temperatures (400 and 800 °C). The values on the plot represent the substrate temperature that is seen by each of the four splats in a pass. For example, the value shown for splat 3 is the surface of the second splat after it has cooled for 10 ms, a time scale that is characteristic of the average time between subsequent splat impacts.[18]

The one-dimensional model results revealed that, after 10 ms, the temperatures of the splat and substrate were uniform to within 5 K over a depth of approximately four splat thicknesses. This depth is approximately the size of the substrate domain required for the two-dimensional remelt analysis. Thus, each subsequent splat in a pass can be modeled in the same manner as the first splat—i.e., with a uniform substrate temperature, but with the higher value shown in Fig. 13.

No additional two-dimensional simulations were carried out for the multiple-splat analysis. Instead, an estimate of the extent of remelt was obtained using the following approach. Values of T_{sub} from the one-dimensional analysis (Fig. 13) were used to calculate U for the second through fourth splats. For example, for the large-scale roughness and an initial substrate temperature of 800 °C, the substrate temperature seen by the second splat, 942 °C, corresponded to a value of U = 0.322. Using these values of U, estimates of R_m were obtained from the remelt curves for small-scale and large-scale roughness. Following the same example, the value of U = 0.322 will result in remelt of 14% for the large-scale roughness and 27% for the small-scale roughness.

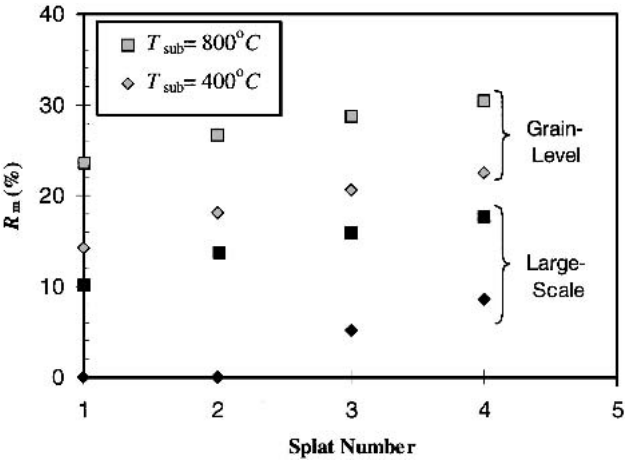

Fig. 14 Results of a multiple-splat analysis for large-scale and grain-level roughness (T_{spl} = 3500 °C; 10 ms between splats)

The results of the multiple-splat analysis are seen in Fig. 14. For the baseline substrate temperature case (800 °C) and the large-scale roughness, the higher substrate temperatures for subsequent splats result in an increase in the extent of remelting, approximately 18% for the fourth splat compared to 10% for the first splat. For the lower substrate temperature, there is no remelting for the first two splats, but substrate remelting is observed for all subsequent splats. The reduced substrate remelting for the first splat for both cases may explain the observation of more intersplat delaminations as compared to the interlamellar delaminations.[2] For the grain-level roughness, the remelt after four splats is over 30% for the case of the 800 °C substrate temperature.

4. Conclusions

A two-dimensional finite element model was developed for studying the dynamics of splat solidification on a rough sub-

strate. Of particular interest is the degree to which the substrate surface is remelted, since that is expected to be related to important coating properties such as cracks, which might explain the grain growth through splat boundaries that is seen in coatings, and is indicative of the local thermal dynamics. Parametric studies were performed to study the effect of substrate temperature, splat temperature, and roughness characteristics on the onset and extent of remelt for zirconia splats on a zirconia substrate. The simulations incorporated the effect of increasing substrate temperatures that are associated with multiple splats in a given pass.

Remelting of the substrate/deposited splats is promoted by the presence of roughness on the surface, a phenomenon not seen with smooth substrates for the conditions studied, indicating that substrate roughness is an important parameter to be incorporated into studies of splat solidification. These results may be significant for understanding the effect of thermal conditions on the development of microstructural features and, hence, on the properties of plasma-sprayed TBCs. In particular, the results are consistent with the observations of a 20% true contact area for zirconia coatings[6] and the dependence of horizontal delaminations on the substrate temperature.[2]

The effects of thermal conditions on remelt (including multiple splat cases) were consolidated into a single nondimensional parameter, $U = (T_{spl} - T_m)/(T_{spl} - T_{sub})$, with the onset of remelt characterized by a nondimensional remelting point, U_{remelt}. Below U_{remelt}, no remelt is observed, while above U_{remelt} the extent of remelt can be approximated by an equation of the form $R_m = C(U - U_{remelt})^{0.5}$. For the small-scale roughness (i.e., submicron), U_{remelt} was lower and C was higher than for the larger scale roughness (i.e., tens of microns), leading to nearly twice the extent of remelt for a given set of conditions.

For conditions that are characteristic of plasma-sprayed zirconia, changing the splat temperature has a greater effect on the extent of remelt than does changing the substrate temperature. However, from a control point of view, the substrate temperature may be more easily changed over a larger temperature range.

Future articles will address extending this analysis to include three dimensions, will report on an experimental analysis of coatings, and will analyze the implications of the results for thermal gradient dynamics during solidification.

Acknowledgments

The material in this article is based on work supported by the National Science Foundation under Grant No. DMI-9713957. The authors would like to acknowledge Dr. Soumendra Basu and graduate students Guosheng Ye and Mohinder Sikka for their discussions, insights, analyses, and sample characterizations.

References

1. M. Vardelle, A. Vardelle, and P. Fauchais: "Influence of Particle Parameters at Impact on Splat Formation and Solidification in Plasma Spraying Processes," *J. Thermal Spray Technol.*, 1994, *4*(1), pp. 50-58.
2. P. Bengtsson and P.T. Johannesson: "Characterization of Microstructural Defects in Plasma-Sprayed Thermal Barrier Coatings," *J. Thermal Spray Technol.*, 1995, *4*(3), p. 245.
3. S. Boire-Lavigne, C. Moreau, and R.G. Saint-Jacques: "The Relationship between the Microstructure and Thermal Diffusivity of Plasma-Sprayed Tungsten Coatings," *J. Thermal Spray Technol.*, 1995, *4*, pp. 261-67.
4. A.S. Houlbert, P. Cielo, C. Moreau, and M. Lamontagne: "Measurement of Thermal Diffusivity and Anisotropy of Plasma-Sprayed Coatings," *Int. J. Thermophys.*, 1994, *15*(3), p. 525.
5. C. Moreau, P. Fargier-Richard, R.J. St. Jacques, and P. Cielo: "Thermal Diffusivity of Plasma-Sprayed Tungsten Coatings," *Surf. Coat. Technol.*, 1993, *61*, pp. 67-71.
6. R. McPherson: "The Relationship between Mechanism of Formation, Microstructure and Properties of Plasma Sprayed Coatings," *Thin Solid Films*, 1981, *83*, pp. 297-310.
7. J.H. Harding, P.A. Mulheran, S. Cirolini, M. Marchese, and G. Jacucci: "Modeling the Deposition Process of Thermal Barrier Coatings," *J. Thermal Spray Technol.*, 1995, *4*, pp. 34-40.
8. S. Kuroda: "The Quenching Stress in Thermally Sprayed Coatings," *Thin Solid Films*, 1991, *200*, pp. 49-66.
9. C. Moreau, M. Lamontagne, and P. Cielo: "Influence of the Coating Thickness on the Cooling Rates of Plasma-Sprayed Particles Impinging on a Substrate," *Surface Coatings Technol.*, 1992, *53*, pp. 107-14.
10. L. Bianchi, A. Denoirjean, F. Blein, and P. Fauchais: "Microstructural Investigation of Plasma-Sprayed Ceramic Splats," *Thin Solid Films*, 1997, *299*, pp. 125-35.
11. G.X. Wang and E.F. Matthys: "Modeling of Heat Transfer and Solidification during Splat Cooling: Effect of Splat Thickness and Splat/Substrate Thermal Contact," *Int J. Rapid Solidification*, 1991, *6*, pp. 141-74.
12. P.G. Boswell: "Solidification Models for High Cooling Rates," *Metals Forum*, 1979, *2*, pp. 40-54.
13. V.V. Sobolev, J.M. Guilemany, and A.J. Martin: "Analysis of Splat Formation during Flattening of Thermally Sprayed Droplets," *Mater. Lett.*, 1996, *29*, pp. 185-90.
14. V.V. Sobolev and J.M. Guilemany: "Influence of Solidification on the Flattening of Droplets during Thermal Spraying," *Mater. Lett.*, 1996, *28*, pp. 71-75.
15. H. Fukanama: "A Porosity Formation and Flattening Model of an Impinging Molten Particle in Thermal Spray Coatings," *J. Thermal Spray Technol.*, 1994, *3*(1), p. 33.
16. L. Bianchi, A.C. Leger, M. Vardelle, A.Vardelle, and P. Fauchais: "Splat Formation and Cooling of Plasma-Sprayed Zirconia," *Thin Solid Films*, 1997, *305*, pp. 35-47.
17. M. Bertagnolli, M. Marchese, and G. Jacucci: "Modeling of Particles Impacting on a Rigid Substrate under Plasma Spraying Conditions," *J. Thermal Spray Technol.*, 1994, *4*(1), pp. 41-49.
18. M. Sikka: "Modeling for Control of Plasma Deposition: Plasma Particle Interactions and Solidification Process," M.S. Thesis, Boston University, College of Engineering, 1997.
19. V.R. Voller, C. Swaminathan, and B. Thomas: "Fixed Grid Techniques for Phase Change Problems: A Review," *Int. J. Num. Meth. Eng.*, 1991, *30*, pp. 875-79.
20. R. Khare: "2-Dimensional Thermal Modeling of Zirconia Splat Solidification on Rough Substrates: Investigation of Remelt and Cooling Rates," M.S. Thesis, Boston University, College of Engineering, Boston, MA, 1999.
21. R.C. Brink: "Material Property Evaluation of Thick Thermal Barrier Coating Systems," *Trans. ASME*, 1989, *111*, pp. 570-77.
22. V.R. Voller and M. Cross: "An Explicit Numerical Method to Track a Moving Phase Change Front," *Int. J. Heat Transfer*, 1983, *26*, pp. 147-50.